

Anelastic spectroscopy study of the spin-glass and cluster spin-glass phases of $\text{La}_{2-x}\text{Sr}_x\text{CuO}_4$ ($0.015 < x < 0.03$)

A. Paolone,¹ F. Cordero,² R. Cantelli,¹ and M. Ferretti³¹Università di Roma "La Sapienza," Dipartimento di Fisica, Piazzale Aldo Moro 2, I-00185 Roma, and INFM, Italy²CNR, Area di Ricerca di Roma-Tor Vergata, Istituto di Acustica "O.M. Corbino," Via del Fosso del Cavaliere 100, I-00133 Roma, and INFM, Italy³Università di Genova, Dipartimento di Chimica e Chimica Industriale, Via Dodecaneso 31, I-16146 Genova, and INFM, Italy

(Received 15 February 2002; revised manuscript received 10 June 2002; published 4 September 2002)

The anelastic spectra of $\text{La}_{2-x}\text{Sr}_x\text{CuO}_4$ have been measured at liquid-He temperatures slightly below and above the concentration $x_c \approx 0.02$, which is considered to separate the spin-glass phase from the cluster spin-glass (CSG) phase. For $x \leq x_c$, all the elastic energy-loss functions show a step below the temperature $T_g(x = 0.02)$ of freezing into the CSG state, similar to what is found in samples well within the CSG phase, but with a smaller amplitude. The excess dissipation in the CSG state is attributed to the motion of the domain walls between the clusters of antiferromagnetically correlated spin. These results are in agreement with the recent proposal, based on inelastic neutron scattering, of an electronic phase separation between regions with $x \sim 0$ and $x \sim 0.02$, at least for $x > 0.015$.

DOI: 10.1103/PhysRevB.66.094503

PACS number(s): 74.25.Ld, 62.40.+i, 74.72.Dn

I. INTRODUCTION

The magnetic properties of the High- T_c Superconductors (HTCS) have attracted much interest also because these compounds are experimental realizations of a two-dimensional (2D) Heisenberg antiferromagnet.¹ In undoped La_2CuO_4 , the Cu^{2+} spins order into a 3D antiferromagnetic (AF) state below $T_N \approx 315$ K with the staggered magnetization in the a - b plane.² When doping by substituting Sr for La, the long-range AF order is rapidly suppressed, and around $x_c \approx 0.02$ the Néel temperature drops to 0 K. In the long-range AF region, $T_N(x)$ follows a power-law relationship with x , interpreted as an indication that the holes introduced by doping form walls separating domains of undoped material.³ Later work indicated that the spin degrees of freedom associated with the doped holes are distinct from the in-plane Cu^{2+} spin degrees of freedom that order themselves below T_N , and the localization of the doped holes allows the associated spins to progressively slow down and freeze.^{1,4} The state in which the doped spins freeze is usually referred to as a spin-glass (SG) state, and occurs below $T_f(x) \approx (815 \text{ K})x$. For $x > x_c$, there is no long-range AF order, but approaching $T_g \approx 0.2 \text{ K}/x$ AF correlations develop within domains separated by charge walls, with the easy axes of the staggered magnetization uncorrelated between different clusters. This picture corresponds to a cluster spin-glass (CSG) state. The formation of the SG and CSG states are inferred from sharp maxima in the ¹³⁹La nuclear quadrupole resonance (NQR) (Refs. 1, 5, and 6), and μSR relaxation rates,⁷ which indicate the slowing of the AF fluctuations below the measuring frequency ($\sim 10^7 - 10^8$ Hz in those experiments), and from the observation of irreversibility, remnant magnetization, and scaling behavior in magnetic-susceptibility experiments.^{8,9} Figure 1 is a schematic representation of the canonical phase diagram of $\text{La}_{2-x}\text{Sr}_x\text{CuO}_4$, including the doping dependences of T_f , T_g , T_N , and the transition temperature T_t from the high-

temperature tetragonal (HTT) to the low-temperature orthorhombic (LTO) phases.

Also anelastic spectroscopy can provide useful information about the magnetic properties of HTCS. Above x_c , the elastic energy-loss coefficient shows a rise below a temperature T_{on} close to the $T_g(x)$ for freezing into the CSG state.^{10,11} The absorption is not peaked near T_g , but is step-like or at least displays a plateau, and therefore does not directly correspond to the peak in the dynamic spin susceptibility due to the spin freezing; rather, it has been attributed to the stress-induced changes of the sizes of the spin clusters, or equivalently to the motion of the domain walls.^{10,11}

Recently, Matsuda *et al.*¹² reported on a neutron-scattering study of the magnetic correlations in $\text{La}_{2-x}\text{Sr}_x\text{CuO}_4$ for $x < x_c$, which suggests a different picture of the spin-glass phase. In fact, they found that also at $x < x_c$, the 3D AF ordered phase coexists below ~ 30 K with domains of "diagonal" stripe phase (with the hole stripes at 45° with respect to the Cu-O bonds), as observed for $x > x_c$. According to these authors, the hole localization starting around 150 K involves an electronic phase separation into regions with $x_1 \sim 0$ and $x_2 \sim 0.02$. The volume fraction of the $x_2 = 0.02$ phase changes as a function of the Sr doping, in order to achieve the average x .

In the following we will report on anelastic spectroscopy measurements of the lightly doped $\text{La}_{2-x}\text{Sr}_x\text{CuO}_4$, where the anelastic spectra for $x < x_c$ present the same features attributed to the domain-wall motion into the CSG phase, although attenuated. The steplike rise of dissipation occurs near 10 K, as for $x \approx 0.02$, supporting the view of an electronic phase separation, at least for $0.015 < x < 0.02$.

II. EXPERIMENT AND RESULTS

The samples were prepared as described in Ref. 13. The specimens were prepared by conventional solid-state reac-

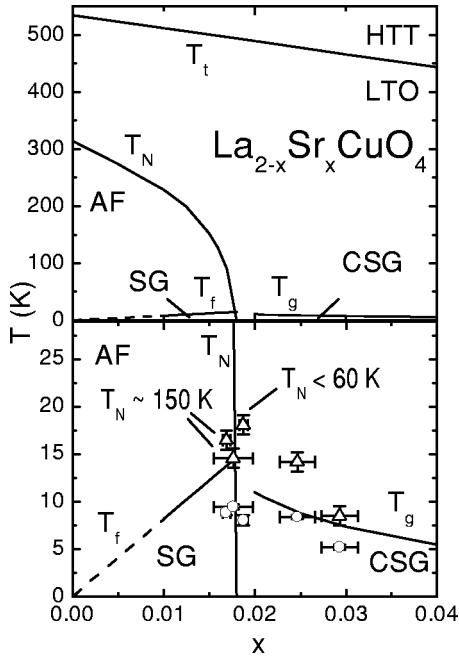


FIG. 1. Schematic phase diagram of $\text{La}_{2-x}\text{Sr}_x\text{CuO}_4$ at low doping. T_f , T_g , T_N , and T_t are obtained according to Ref. 15. The open circles and triangles represent T_{on} (see text) and the temperature of the minimum of the derivatives of the Q^{-1} curves (see Fig. 4) for the samples studied in this work. Their T_N values according to Ref. 18 are also reported.

tions at 1000 °C using stoichiometric amounts of high-purity oxides, La_2O_3 , CuO , and SrO_2 . Precursor powders were carefully mixed in a ball mill in agate jars under ethanol for approximately 1 h. After drying, the mixture was isostatically pressed into rods at room temperature, placed in a Al_2O_3 boat, and put into a hot furnace in air at the synthesis temperature between 1080 and 1130 °C, depending on doping. The sinterized samples were cut in bars of approximately $40 \times 4 \times 0.6 \text{ mm}^3$. In the as-sintered state all the samples contained small amounts of interstitial O that was outgassed by heating in vacuum up to 790 K. The complex Young's modulus $E(\omega) = E' + iE''$, whose reciprocal is the elastic compliance $S = E^{-1}$, was measured as a function of temperature by electrostatically exciting the flexural modes. The vibration amplitude was detected by a frequency modulation technique. The vibration frequency $\omega/2\pi$ is proportional to $\sqrt{E'}$, while the elastic energy-loss coefficient (or reciprocal of the mechanical Q) is given by $Q^{-1}(\omega, T) = E''/E' = S''/S'$,¹⁴ and was measured by the decay of the free oscillations or the width of the resonance peak. The imaginary part of the dynamic susceptibility S'' is related to the spectral density $J_\varepsilon(\omega, T) = \int dt e^{i\omega t} \langle \varepsilon(t) \varepsilon(0) \rangle$ of the macroscopic strain ε through the fluctuation-dissipation theorem, $S'' \propto (\omega/2k_B T) J_\varepsilon$.

In general, any elementary relaxation process with a thermally activated relaxation time $\tau(T)$ contributes with $S'' \propto \omega\tau/[1 + (\omega\tau)^2]$, peaked at the temperature at which $\omega\tau = 1$ (which therefore increases with increasing ω). In principle, also the slowing down of the magnetic fluctuations toward the spin-glass freezing, which give rise to the sharp

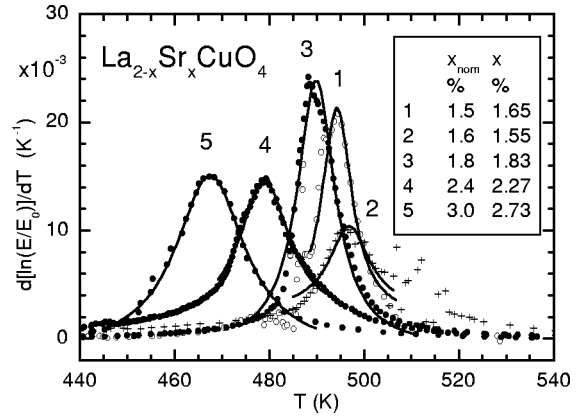


FIG. 2. Derivatives of the logarithm of the Young's modulus with respect to temperature at the HTT/LTO transformation for the five samples studied here. The inset shows the nominal doping and the doping level deduced from the temperature of the transition.

maxima in the ^{139}La NQR relaxation rates, may produce narrow peaks in the elastic energy-loss function if the spin fluctuations cause strain fluctuations through magnetoelastic coupling.¹⁰ However, in the samples with $x > 0.02$ the transition to the cluster spin-glass state is detected in the anelastic spectra by large steplike features in Q^{-1} , which cannot be explained by this mechanism. It has been proposed that the main contribution to these features comes from the stress-induced movement of the boundaries between the clusters of quasifrozen antiferromagnetically correlated spins.¹⁰ This effect is well known for ferromagnetic materials¹⁴ with an anisotropic magnetoelastic strain coupled with the magnetization axis. The application of an external stress (due to the sample vibration) changes the elastic energies of the domains according to the relative orientation of the stress and of the magnetization axis; consequently, the domains with lower elastic energy grow at the expenses of the others, or equivalently the domain walls move. The same mechanism is possible also for an ordered AF state or for glassy states consisting of antiferromagnetically correlated clusters, if there is an anisotropic magnetoelastic strain with the principal axes oriented according to the direction of the staggered magnetization. The dynamics of the domain boundaries is different from that of the critical or freezing fluctuations and generally produces broad peaks in the susceptibilities, like those presented in Q^{-1} .

The nominal compositions of the samples were: $x_{\text{nom}} = 0.015, 0.016, 0.018, 0.024, \text{ and } 0.030$. The final Sr contents were checked from the temperature positions of the steps in the Young's modulus E , and of the elastic energy-loss function Q^{-1} , due to the HTT/LTO transition, which occurs at a temperature $T_t(x)$ decreasing with doping approximately as $T_t(x) = (535 - x/0.217) \text{ K}$ (Ref. 15). The shapes of the anomaly in E and of the step in Q^{-1} cannot be completely fitted by a simple model, since they include both contributions from the coupling of the spontaneous strain with the soft mode¹⁶ and from the domain-wall motion,¹⁷ but its position in temperature provides information about the level of doping. Figure 2 presents the logarithmic derivative of the Young's modulus with respect to temperature,

$d\ln[E/E(0)]/dT$, so that the steps become peaks whose widths provide upper limits to the spread of the local Sr concentration; the peaks are fitted with lorentzians. The Sr concentrations estimated from the peak positions and from $T_i(x)$ are $x = 0.0165, 0.0155, 0.0183, 0.0227$, and 0.0273 , respectively; the sample with $x_{\text{nom}} = 0.016$ results to be less doped than the one with $x_{\text{nom}} = 0.015$ and with a broader transition. There is considerable overlapping of the peaks of the samples with $x_{\text{nom}} < 0.02$, but this should not be simply interpreted as a distribution of local x spanning 0.015–0.018 for all these samples. In fact, the peaks in the derivative of $E(T)$ cannot be interpreted as the distribution function of the local x after the T scale is converted into an x scale inverting $T_i(x)$, since the step of $E(T)$ has an intrinsic width due to the progressive phonon softening above T_i and to the relaxational character of the domain-wall motion below T_i . The undoped samples, for example, certainly do not have a spread of Sr concentration, but the widths of their lorentzians (not shown here) are 16–22 K, compared to 10 K of the sample with $x_{\text{nom}} = 0.016$.

Also the position of the steps of the elastic energy-loss function due to the HTT/LTO transition can be used to estimate the Sr doping of the samples. However, it seems to us that the criterion for the location of these feature is more arbitrary than that described in the previous paragraph for the location of the steps in the Young's modulus E . The Sr concentrations obtained with this second method using the doping dependence of $T_i(x)$ are $x = 0.0173, 0.0198, 0.0192, 0.0266$, and 0.0313 .

A further characterization of the samples with $x_{\text{nom}} < 0.02$ is provided by measurements of the Néel temperature T_N , by means of NQR and superconducting quantum interference device measurements performed by different authors on the same samples used in this work. The T_N of the samples with $x_{\text{nom}} = 0.015$ and 0.016 was ~ 150 K for both samples.¹⁸ In the case of the sample with $x_{\text{nom}} = 0.018$ it was not possible to obtain an estimation of T_N , as the intense feature usually attributed to spin freezing is superimposed on the peak due to the Néel transition in the ^{139}La relaxation rate $2W$ spectrum.¹⁸ This experiment sets an upper limit to T_N of ~ 60 K.

Despite the uncertainties in the Sr composition of the samples, combining the results obtained from our anelastic spectroscopy measurements with those of the NQR study, one can be sure that at least the samples with $x_{\text{nom}} = 0.015$ and 0.016 belong to the region of the phase diagram where a SG phase is expected at low temperature. For the sample with $x_{\text{nom}} = 0.018$ there are strong indications from the anelastic spectroscopy measurements here reported that the real doping is lower than $x = 0.02$. In the following, to avoid confusion, we will refer to the doping level obtained from the position of the step in the Young's modulus, which provides a less arbitrary criterion to estimate x .

Figure 3 presents the anelastic spectra of the five samples measured exciting the first flexural mode, around 1 kHz. The sharp rise of dissipation at the lowest temperatures is the tail of an intense peak attributed to the tunneling-driven tilt motion of a fraction of the O octahedra.^{19,20} The shift of the

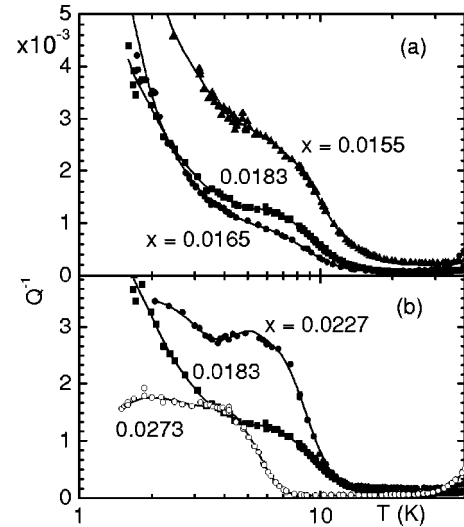


FIG. 3. Elastic energy-loss coefficient of $\text{La}_{2-x}\text{Sr}_x\text{CuO}_4$ with $x = 0.0165$ (1.35 kHz), $x = 0.0183$ (1.05 kHz), and $x = 0.0155$ (0.76 kHz) in part (a) of the figure and with $x = 0.0227$ (0.97 kHz) and $x = 0.0273$ (1.72 kHz) in part (b).

peak to lower temperature with increasing doping would be due to a direct coupling between the hole excitations and the tunneling-driven local tilts of the O octahedra: the more the hole excitations, the faster the local tilting.²⁰ We are concerned with the steplike feature at $T_g(x) \approx 0.2/x$ for $x > 0.02$, and below ≈ 10 K for $x < 0.02$. That such a dissipation rise occurs at T_g and is steplike or at least consists of a plateau rather than a peak is particularly evident at higher doping, when the influence of the tail of the peak at lower temperature is less important;¹⁰ here only two curves with $x \geq 0.02$ are presented. As already reported, the dissipation rise has been attributed to the stress-induced movement of the boundaries between the clusters of quasifrozen antiferromagnetically correlated spins which form the CSG phase.¹⁰ The main result is that also the samples with $x < 0.02$ present a similar feature around 10 K. With lowering x below 0.02, the position of the dissipation step remains unchanged, while its intensity decreases; this is more difficult to see for the sample with $x = 0.0155$, since the tail of the low-temperature peak is shifted to higher temperature (consistent with the lowest doping in spite of the nominal x). Taking into account also the previous data,¹⁰ it appears that, starting from high doping and lowering it, the dissipation step first rises in temperature according to $T_g(x)$ and increases in intensity down to $x \approx 0.02$; on doping below that, its temperature remains unchanged and the intensity decreases.

III. DISCUSSION

One would expect that the dissipation rise near 10 K for $x < 0.02$ corresponds to the peak in the spin susceptibility occurring when the magnetic fluctuations slow down below the measuring frequency during the freezing process into the SG phase, as in the NQR measurements;^{1,5,6} also the temperature region would be as expected, since, according to the

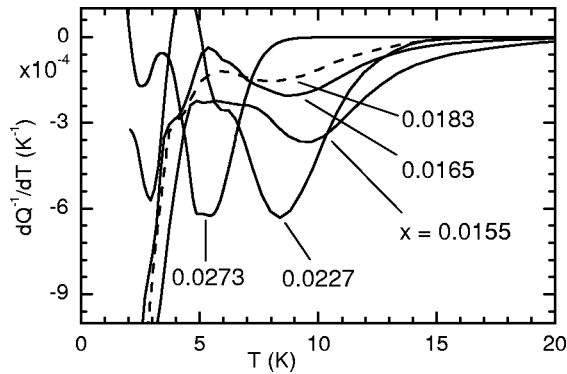


FIG. 4. Derivative of the elastic energy loss with respect to temperature for the five samples studied here.

generally accepted phase diagram,¹⁵ at $x = x_c$ both $T_f(x)$ and $T_g(x)$ merge at 10–15 K. However, there are two features signaling the different nature of the absorption rise below ~ 10 K: one is the shape, certainly different from the sharp peak of the NQR relaxation rate, and the other is the total absence of the expected linear shift towards lower temperature when the doping is reduced. This is better demonstrated by the derivatives of the $Q^{-1}(T)$ curves in Fig. 4, where the negative peaks at high temperature, labeled with the estimated doping values, correspond to the steps in $Q^{-1}(T)$. The three peaks with $x < 0.02$ even shift to higher temperature with decreasing x , although the effect is very small and most likely attributable to the increasing influence of the tail of the peak at lower temperature. Instead, according to the generally adopted phase diagram with $T_f(x) \approx x(815 \text{ K})$ the three peaks should display an overall shift by 2.3 K in the opposite direction; it is therefore clear from Fig. 4 that there is no relation between the acoustic dissipation step and $T_f \propto x$.

The spectra of the samples with $x < 0.02$ strictly resemble those for $x > 0.02$, and the latter have been successfully interpreted in terms of onset below T_g of the motion of the domain walls between different spin clusters in the CSG phase. The decrease of the amplitude Δ of the absorption step above $x = 0.02$ has been semiquantitatively explained considering a simple model of the CSG phase, with the Sr atoms acting as pinning points for the domain walls, which coincide with the hole stripes.²¹ The relaxation strength is expected to be of the form $\Delta \propto nl^\alpha$, where n is the volume concentration of the domain walls, l is the distance between pinning points, and α turns out to be ≈ 2.5 , intermediate between the case of the motion of dislocations and of walls between ferromagnetic domains.²¹ It was also possible to observe the pinning of the walls by the low-temperature tetragonal lattice modulation in samples doped with Ba instead of Sr.²¹ The mechanism of dissipative motion of the domain walls cannot be applied to the SG state, even admitting the existence of hole stripes below 10 K, since they would move into a uniform long-range ordered AF matrix, instead of separating inequivalent domains, so that they would not produce any change of the anelastic strain and consequently would not contribute to the elastic energy-loss function.

It has to be concluded that the anelastic spectra for $x < 0.02$ [Fig. 3(a)] cannot be justified in terms of the spin-

glass phase with $T_f(x)$ increasing linearly with x ; rather, they can be explained in a straightforward way within the physical picture derived from the inelastic neutron-scattering measurements.¹² According to these observations, there is an electronic phase separation below $x = 0.02$, where domains with fixed $x_2 = 0.02$ coexist with regions of undoped material with $x_1 = 0$. Such domains have sizes estimated in several hundreds of angstroms within the CuO_2 planes, and display the same “diagonal stripe” correlations that are observed in the CSG state for $x \geq 0.02$. The volume fraction of these domains has also been verified to increase linearly with x , as expected. In this phase-separation picture, the elastic energy dissipation curves for $x < 0.02$ simply contain the steplike increase due to the motion of the hole stripes within the $x_2 \approx 0.02$ domains, whose sizes are sufficiently large that they appear as the homogeneous phase $x = 0.02$ with the same $T_g \approx 10$ K. The reduced volume fraction at lower doping simply results in a reduced amplitude of the elastic energy absorption.

The fact that the temperature at which our measurements reveal the presence of spin domains is much lower than the temperature of 30 K reported by Matsuda *et al.*¹² also agrees with what is observed in the CSG state.¹¹ In fact, the onset temperature for freezing toward the glass state, T_{on} , depends on the time scale at which the experimental technique probes the system, and decreases as the angular frequency ω of the probe decreases. In neutron-scattering experiments ω is of the order of $4 \times 10^{11} \text{ s}^{-1}$, while for the anelastic spectroscopy $\omega \sim 10^4 - 10^5 \text{ s}^{-1}$, resulting in a factor of 2.5 between the two T_{on} 's at $x \sim 0.03$;¹¹ this is consistent with the $T_{on} = 10 - 15 \text{ K}$ deduced from the curves of Fig. 3(a).

The dissipation curves of Fig. 3(a) clearly indicate that the same dissipation mechanism of the CSG phase is operative also at $x < 0.02$, and therefore are in good agreement with the phase-separation picture from the neutron-scattering experiment;¹² however, these curves alone are not sufficient for clearly discriminating between a neat phase separation into $x_1 \sim 0$ and $x_2 \sim 0.02$ or a situation with a smooth transition from the CSG to the SG state over a wide concentration range around 0.02. For example, according to the theoretical model proposed by Gooding *et al.*,²² at low temperature the holes localize near the Sr dopants and circulate over the four Cu atom neighbors to Sr, inducing a distortion of the surrounding Cu spins, otherwise aligned according to the prevalent AF order parameter. The spin texture arising from the frustrated combination of the spin distortions from the various localized holes produces domains with differently oriented AF order parameters, which can be identified with the frozen AF spin clusters. In this model there is no clear boundary between the SG and CSG states, and the present data could also fit into such a description.

The possibility has also to be considered that the discrepancy between the present results below $x \approx 0.02$ and the canonical phase diagram is due to inhomogeneous doping of the samples at a microscopic level. Errors in evaluating the actual doping and inhomogeneous doping would produce particularly large shifts and uncertainty in the determination of T_f and T_g , since these temperatures appear to merge

around the value 10–15 K at $x=x_c=0.02$, where they strongly depend on doping. Indeed, there is a wide scattering of experimental data in that region of the phase diagram,^{15,23} which can be due to uncertainties in x , but also to the fact that the transition between SG and CSG is not as sharp as supposed. The present data support the second explanation. In fact, we cannot exclude the possibility of inhomogeneous doping of our samples with certainty, only based on the width of the HTT/LTO phase transition, because we are not able to carry out a rigorous analysis of the curves of Fig. 2. Still, we note that if the high temperature of the step of samples with average $x<0.02$ is due to regions with $x>0.02$, then we should expect a similar spread of the local doping also for the samples with $x>0.02$, since all the samples have been prepared in the same way. Then, the sample with $x=0.0273$ should exhibit a partial onset of dissipation already above 10 K, due to regions with $x\approx 0.02$. The sample with $x=0.0273$, instead, displays a neat rise below 8 K, excluding the presence of regions with $x\approx 0.02$. It can be concluded that the present measurements demonstrate the presence of CSG domains also for $x<0.02$, and the insensitivity of the temperature of the acoustic anomaly on doping supports the proposal¹² of an intrinsic phase separation at $x<0.02$.

IV. CONCLUSION

We measured the anelastic spectra of $\text{La}_{2-x}\text{Sr}_x\text{CuO}_4$ for both $x<0.02$ and $x>0.02$, spanning the region of the phase diagram where the transition from the SG to the CSG phase is expected. The same steplike feature in the elastic energy-loss function that has been attributed to the domain-wall motion in the CSG state is also found for $0.015<x<0.02$. The step cannot be related to the SG phase whose onset is usually assumed to be $T_f\propto x$, since its temperature remains locked at the value found for $x=0.02$. The present data clearly show that CSG regions exist also for $x<0.02$ and therefore there is no neat separation between the SG and CSG regions. They can be naturally interpreted in the framework of the phase-separation model for $x<0.02$, recently proposed by Matsuda *et al.*¹² to explain the inelastic neutron-scattering measurements.

ACKNOWLEDGMENTS

The authors thank Professor A. Rigamonti for useful discussions. This work was done in the framework of the Advanced Research Project SPIS of INFN.

-
- ¹A. Rigamonti, F. Borsa, and P. Carretta, *Rep. Prog. Phys.* **61**, 1367 (1998).
- ²D. Vagnin, S.K. Sinha, D.E. Moncton, D.C. Johnston, J.M. Newsam, C.R. Safinya, and H.E. King, Jr., *Phys. Rev. Lett.* **58**, 2802 (1987).
- ³J.H. Cho, F.C. Chou, and D.C. Johnston, *Phys. Rev. Lett.* **70**, 222 (1993).
- ⁴F.C. Chou, F. Borsa, J.H. Cho, D.C. Johnston, A. Lascialfari, D.R. Torgeson, and J. Ziolo, *Phys. Rev. Lett.* **71**, 2323 (1993).
- ⁵J.H. Cho, F. Borsa, D.C. Johnston, and D.R. Torgeson, *Phys. Rev. B* **46**, 3179 (1992).
- ⁶M.-H. Julien, F. Borsa, P. Carretta, M. Horvatic, C. Berthier, and C.T. Lin, *Phys. Rev. Lett.* **83**, 604 (1999).
- ⁷Ch. Niedermayer, C. Bernhard, T. Blasius, A. Golnik, A. Moodenbaugh, and J.I. Budnick, *Phys. Rev. Lett.* **80**, 3843 (1998).
- ⁸F.C. Chou, N.R. Belk, M.A. Kastner, R.J. Birgeneau, and A. Aharony, *Phys. Rev. Lett.* **75**, 2204 (1995).
- ⁹S. Wakimoto, S. Ueki, Y. Endoh, and K. Yamada, *Phys. Rev. B* **62**, 3547 (2000).
- ¹⁰F. Cordero, A. Paolone, R. Cantelli, and M. Ferretti, *Phys. Rev. B* **62**, 5309 (2000).
- ¹¹R.S. Markiewicz, F. Cordero, A. Paolone, and R. Cantelli, *Phys. Rev. B* **64**, 054409 (2001).
- ¹²M. Matsuda, M. Fujita, K. Yamada, R.J. Birgeneau, Y. Endoh, and G. Shirane, *Phys. Rev. B* **65**, 115202 (2002).
- ¹³M. Napoletano, J.M. Gallardo Amores, E. Magnone, G. Busca, and M. Ferretti, *Physica C* **319**, 229 (1999).
- ¹⁴A.S. Nowick and B.S. Berry, *Anelastic Relaxation in Crystalline Solids* (Academic Press, New York, 1972).
- ¹⁵D.C. Johnston, in *Handbook of Magnetic Materials*, edited by K.H.J. Buschow (North-Holland, Amsterdam, 1997), p. 1.
- ¹⁶J.L. Sarrao, D. Mandrus, A. Migliori, Z. Fisk, I. Tanaka, H. Kojima, P.C. Canfield, and P.D. Kodali, *Phys. Rev. B* **50**, 13 125 (1994).
- ¹⁷W.-K. Lee, M. Lew, and A.S. Nowick, *Phys. Rev. B* **41**, 149 (1990).
- ¹⁸M. Corti and A. Rigamonti (private communication).
- ¹⁹F. Cordero, C.R. Grandini, G. Cannelli, R. Cantelli, F. Trequatrin, and M. Ferretti, *Phys. Rev. B* **57**, 8580 (1998).
- ²⁰F. Cordero, R. Cantelli, and M. Ferretti, *Phys. Rev. B* **61**, 9775 (2000).
- ²¹F. Cordero, A. Paolone, R. Cantelli, and M. Ferretti, *Phys. Rev. B* **64**, 132501 (2001).
- ²²R.J. Gooding, N.M. Salem, R.J. Birgeneau, and F.C. Chou, *Phys. Rev. B* **55**, 6360 (1997).
- ²³A. Campana, R. Cantelli, F. Cordero, M. Corti, and A. Rigamonti, *Eur. Phys. J. B* **18**, 49 (2000).